PROCEEDINGS OF SCIENCE

Non-standard interactions and the $\tau^- \to (K\pi)^-\nu_\tau$ decays

Javier Rendón[a,*]

[a] *Cinvestav,*
Apdo. Postal 14-740, 07000 Ciudad de México, México

E-mail: jrendon@fis.cinvestav.mx

In this work we study the decays $\tau^- \to (K\pi)^-\nu_\tau$ using an effective field theory constructed with dimension six operators with the SM degrees of freedom. The explicit framework is the SMEFT at low energies. Following this framework we have obtained three main results:
(i) we have confirmed that it is impossible to understand the BaBar CP anomaly associated with the channel $\tau \to K_S\pi\nu_\tau$. We have found an upper bound for the NP contribution slightly larger than in Phys. Rev. Lett. 120(2018) no.14, 141803, but still irrelevant compared to the experimental uncertainty by four orders of magnitude approximately;
(ii) we have shown that the bump present in the spectrum measured by the Belle experiment for the $K_S\pi^-$ invariant mass distribution near the threshold cannot be explained by heavy NP;
(iii) we constrain the NP scalar and tensor effective couplings using the decays $\tau^- \to (K\pi)^-\nu_\tau$ and we find that they are competitive with other traditional low energy probes like hyperon decays for the scalar and tensor cases and kaon decays for tensorial interactions (we cannot compete for the case of non-standard scalar interactions in Kaon (semi)leptonic decays).
Besides these three main results, we have also studied the effect of NP in several interesting observables like Dalitz plots, decay spectrum and forward-backward asymmetry. All these observables were calculated in the SM case as well, in order to be able to compare the way in which NP could manifest.

**** 10th International Workshop on Charm Physics (CHARM2020), ****
**** 31 May - 4 June, 2021 ****
**** Mexico City, Mexico - Online ****

*Speaker

PoS(CHARM2020)045

1. Introduction

This work is based in an article that we published recently, for more details see ref. [1].

It is a well known fact that Tau physics is a powerful tool for precision electroweak studies and also a clean low energy QCD laboratory. In this work our purpose is to show that Tau physics is also a very useful probe to study potential NP effects. In particular we want to show how it can be used to study the effects induced by heavy NP in the following observables:

- Check the results in ref. [2], which disprove earlier claims [3–5] that tensor interactions could explain the BaBar CP anomaly in $\tau \to K_S\pi\nu_\tau$ decays [6]. This corresponds to the measurement of A_{CP}, defined in the following way:

$$A_{CP} = \frac{\Gamma(\tau^+ \to \pi^+ K_S \bar{\nu}_\tau) - \Gamma(\tau^- \to \pi^- K_S \nu_\tau)}{\Gamma(\tau^+ \to \pi^+ K_S \bar{\nu}_\tau) + \Gamma(\tau^- \to \pi^- K_S \nu_\tau)} = -3.6(2.3)(1.1) \times 10^{-3}, \tag{1}$$

  which disagrees remarkably with the SM prediction $A_{CP} = 3.32(6) \times 10^{-3}$, driven by neutral kaon mixing [7, 8], probed with high accuracy in semileptonic kaon decays [9]. In fact, the SM prediction is slightly modified by the experimental conditions corresponding to the reconstruction of the K_S at the B-factory, yielding $A_{CP} = 3.6(1) \times 10^{-3}$ [10], which increases the discrepancy at the 2.8 σ level. As a novelty of our treatment, we will discuss the uncertainty induced on A_{CP} by the error of the tensor form factor modulus, while for its phase uncertainty we will follow ref. [2]. This point is extremely important because the CP violation present in the SM [11] is clearly insufficient to understand the baryon asymmetry of the universe [12–14] so that any hint of NP involving CP violation becomes a candidate for providing with a clue to understand the enormous matter-antimatter imbalance. With respect to this BaBar anomaly, however, the related Belle measurement [15] of a binned CP asymmetry in the same decay channel analyzing the decay angular distributions is compatible with zero, as expected in the SM with a permille level precision. An explanation of this discrepancy is needed, and this is precisely one of the goals of this work.

- Three data points at the beginning of the $K_S\pi^-$ spectra measured by Belle [16] have been excluded from the reference fits or signalled as controversial in the dedicated analyses [17–23, 55] and are at variance with the prediction [25]. To our knowledge, only Ref. [26] was able to describe these data points due to the effect on the scalar form factor of the longitudinal correction to the $K^*(892)$ propagator induced by flavor symmetry breaking [1]. We will study if it is possible to explain these conflicting data points by the most general description of heavy NP contributions modifying the $\tau^- \to \bar{u}s\nu_\tau$ decays in the SM.

- Within an effective field theory analysis of possible non-standard charged current interactions, semileptonic tau decays [27–29] have been proved competitive with the traditional semileptonic decays involving light quarks [30–40], like nuclear beta or leptonic and radiative pion decays. In this context, for the Cabibbo-suppressed sector, hyperon semileptonic decays

[1] As we will recall in section 4, the scalar form factor contribution that we employ [56] was obtained as a result of analyzing strangeness-changing meson-meson scattering [57] within Chiral Perturbation Theory [43, 44] with resonances [45, 46], accounting for the leading flavor symmetry breaking.

[34, 37] cannot compete with (semi)leptonic Kaon decays [36], given the (very accurately measured) dominant branching fractions of the latter and the suppressed ones (at most at the permille level) of the former. This intuitive reasoning suggests that strangeness-changing tau decays can also give non-trivial bounds on non-standard charged current interactions, although it is not likely that at a competitive level with $K_{\ell(2,3)}$ decays (however, if we restrict to tensor interactions only, we will see that our couplings are competitive with the ones coming from $K_{\ell(2,3)}$ decays). The present work will make these statements precise.

2. Effective theory analysis of $\tau^- \to \nu_\tau \bar{u} s$

The lepton number conserving effective Lagrangian density constructed with dimension six operators and invariant under the local $SU(3)_C \otimes SU(2)_L \otimes U(1)_Y$ SM gauge group has the following form [41, 42],

$$\mathcal{L}^{(eff)} = \mathcal{L}_{SM} + \frac{1}{\Lambda^2}\sum_i \alpha_i O_i \longrightarrow \mathcal{L}_{SM} + \frac{1}{v^2}\sum_i \hat{\alpha}_i O_i\,, \tag{2}$$

with $\hat{\alpha}_i = (v^2/\Lambda^2)\alpha_i$ the dimensionless couplings encoding NP at a scale of some TeV. Note that we have not included the Weinberg operator which has dimension five since it does not contribute to our processes. The Weinberg operator changes the lepton number in two units ($\Delta L = 2$) and lepton number violation is not present in our decays.

We can explicitly construct the leading low-scale $O(1\text{ GeV})$ effective Lagrangian (which has $SU(3)_C \otimes U(1)_{em}$ local gauge symmetry) for the strangeness-changing semi-leptonic transitions upon integrating out the heavy degrees of freedom [30, 31],

$$\begin{aligned}\mathcal{L}_{cc} =& \frac{-4G_F}{\sqrt{2}} V_{us}\Big[(1+[v_L]_{\ell\ell})\bar{\ell}_L\gamma_\mu\nu_{\ell L}\bar{u}_L\gamma^\mu s_L + [v_R]_{\ell\ell}\bar{\ell}_L\gamma_\mu\nu_{\ell L}\bar{u}_R\gamma^\mu s_R \\ &+ [s_L]_{\ell\ell}\bar{\ell}_R\nu_{\ell L}\bar{u}_R s_L + [s_R]_{\ell\ell}\bar{\ell}_R\nu_{\ell L}\bar{u}_L s_R \\ &+ [t_L]_{\ell\ell}\bar{\ell}_R\sigma_{\mu\nu}\nu_{\ell L}\bar{u}_R\sigma^{\mu\nu}s_L\Big] + \text{h.c.}\,,\end{aligned} \tag{3}$$

where G_F is the tree-level definition of the Fermi constant, $L(R)$ stand for left(right)-handed chiral projections and $\sigma^{\mu\nu} = i\,[\gamma^\mu, \gamma^\nu]\,/2$. Note that if we set $v_L = v_R = s_L = s_R = t_L = 0$, we recover the SM Lagrangian for the strangeness-changing semileptonic tau decays, with momentum transfer much smaller than the M_W scale. Right-handed and wrong-flavor neutrino contributions were neglected in equation (3) since they do not interfere with the SM amplitudes and do not contribute at leading order in the NP effective coefficients.

Besides Lorentz invariance, the only assumptions behind eq. (3) are the local gauge symmetries at low-energies ($U(1)_{em}$ and $SU(3)_C$ of electrodynamics and chromodynamics, respectively) and the absence of light non-SM particles.

It is convenient to recast the spin-zero contributions in terms of currents with defined parity (scalar and pseudoscalar) in the following way

$$\begin{aligned}\mathcal{L}_{cc} =& -\frac{G_F V_{us}}{\sqrt{2}}(1+\epsilon_L+\epsilon_R)\Big[\bar{\tau}\gamma_\mu(1-\gamma_5)\nu_\ell\cdot\bar{u}[\gamma^\mu - (1-2\hat{\epsilon}_R)\gamma^\mu\gamma_5]s \\ &+ \bar{\tau}(1-\gamma_5)\nu_\ell\cdot\bar{u}[\hat{\epsilon}_s - \hat{\epsilon}_p\gamma_5]s + 2\hat{\epsilon}_T\bar{\tau}\sigma_{\mu\nu}(1-\gamma_5)\nu_\ell\cdot\bar{u}\sigma^{\mu\nu}s\Big] + \text{h.c.}\,,\end{aligned} \tag{4}$$

where: $\epsilon_{L,R} = v_{L,R}$, $\epsilon_s = s_L + s_R$, $\epsilon_p = s_L - s_R$, and $\epsilon_T = t_L$. In eq. (4) we have particularized the Lagrangian for the tau lepton case ($\ell = \tau$), and we have also introduced the convenient notation $\hat{\epsilon}_i = \epsilon_i/(1 + \epsilon_L + \epsilon_R)$ [27] for $i = R, S, P, T$ [2]. In this way, our Lagrangian in eq. (4) is equivalent to the one in eq. (9) of Ref. [2] working at linear order in the epsilon Wilson coefficients.

3. Semileptonic τ decay amplitude

In this section we calculate the decay amplitudes corresponding to the $\tau^- \to \bar{K}^0\pi^-\nu_\tau$ and the $\tau^- \to K^-\pi^0\nu_\tau$ decays. The first thing to note is that due to the parity of pseudoscalar mesons, only the vector, scalar and tensor currents give a non-zero contribution to the decay amplitude, as shown in the following equation [3] [4]

$$\begin{aligned}\mathcal{M} =& \mathcal{M}_V + \mathcal{M}_S + \mathcal{M}_T \\ =& \frac{G_F V_{us}\sqrt{S_{EW}}}{\sqrt{2}}(1 + \epsilon_L + \epsilon_R)[L_\mu H^\mu + \hat{\epsilon}_S L H + 2\hat{\epsilon}_T L_{\mu\nu} H^{\mu\nu}],\end{aligned} \tag{5}$$

where the leptonic currents have the following structure (p and p' are the momenta of the tau lepton and its neutrino, respectively),

$$\begin{aligned}L_\mu &= \bar{u}(p')\gamma_\mu(1 - \gamma_5)u(p), \\ L &= \bar{u}(p')(1 + \gamma_5)u(p), \\ L_{\mu\nu} &= \bar{u}(p')\sigma_{\mu\nu}(1 + \gamma_5)u(p),\end{aligned} \tag{6}$$

and the vector, scalar and tensor hadronic matrix elements for the case of the $\tau^- \to \bar{K}^0\pi^-\nu_\tau$ decay, are defined as follows

$$H^\mu = \langle \pi^- \bar{K}^0 | \bar{s}\gamma^\mu u | 0\rangle = Q^\mu F_+(s) + \frac{\Delta_{K\pi}}{s} q^\mu F_0(s), \tag{7}$$

$$H = \langle \pi^- \bar{K}^0 | \bar{s} u | 0\rangle = F_S(s), \tag{8}$$

$$H^{\mu\nu} = \langle \pi^- \bar{K}^0 | \bar{s}\sigma^{\mu\nu} u | 0\rangle = i F_T(s)(p_K^\mu p_\pi^\nu - p_\pi^\mu p_K^\nu), \tag{9}$$

where $q^\mu = (p_\pi + p_K)^\mu$, $Q^\mu = (p_K - p_\pi)^\mu - \frac{\Delta_{K\pi}}{s} q^\mu$, $s = q^2$, and $\Delta_{ij} = m_i^2 - m_j^2$.

The hadron matrix elements H, H^μ and $H^{\mu\nu}$ were decomposed in terms of the allowed Lorentz structures, taking into account the discrete symmetries of the strong interactions, and a number of scalar functions of the invariant mass of the $K\pi$ system: the $F_S(s)$, $F_+(s)$, $F_0(s)$ and $F_T(s)$ form factors; which encode the details of the hadronization process.

[2] We note that this reshuffling is not convenient when comparing neutral and charged current processes and also when analyzing different semileptonic tau decays with an odd and an even number of pseudoscalar mesons, respectively [29]. Since $\epsilon_i = \hat{\epsilon}_i$ at linear order in these coefficients, we may use ϵ_i instead of $\hat{\epsilon}_i$ when comparing to works which use the former instead of the latter.

[3] Eq.(5) displays clearly that the renormalization scale dependence of the Wilson coefficients $\hat{\epsilon}_i$ needs to be cancelled by the one of the hadron matrix elements. As it is conventional, both are defined in the $\overline{MS}$ scheme at $\mu = 2$ GeV.

[4] For convenience, the short-distance electroweak correction factor S_{EW} [47–54] is written as an overall constant, although it only affects the SM contribution. The error of this simplification is negligible working at leading order in the $\hat{\epsilon}_i$ coefficients [27, 28].

The $\tau^- \to K^-\pi^0\nu_\tau$ decay is completely analogous. Neglecting (tiny) isospin corrections, the only difference is given by the Clebsch-Gordan flavor symmetry factor of $\sqrt{2}$ between both decay channels, that is $\sqrt{2}F_{0,+,T}^{K^-\pi^0}(s) = F_{0,+,T}^{\bar{K}^0\pi^-}(s)$.

From equations (6) one can easily see that the vector and the scalar currents are related through the Dirac equation, to see this, let us multiply the leptonic vector current by q^μ

$$\begin{aligned} q^\mu L_\mu &= q^\mu \bar{u}(p')\gamma_\mu(1-\gamma^5)u(p) \\ &= (p_\tau - p_\nu)\bar{u}(p')\gamma_\mu(1-\gamma^5)u(p) \\ &= \bar{u}(p')(\not{p}_\tau - \not{p}_\nu)(1-\gamma^5)u(p) \\ &= \bar{u}(p')(1+\gamma^5)M_\tau u(p)\,, \end{aligned} \tag{10}$$

therefore, we find the following relation

$$L = \frac{L_\mu q^\mu}{M_\tau}\,. \tag{11}$$

Similarly, one can find a relation between the vector and the scalar hadronic matrix elements by taking the four-divergence of equation (7). This yields

$$F_S(s) = \frac{\Delta_{K\pi}}{m_s - m_u}F_0(s)\,. \tag{12}$$

Taking into account the previous two equations, we conclude that the scalar and vector contributions in eq. (5) can be treated jointly by doing the convenient replacement

$$\frac{\Delta_{K\pi}}{s} \to \frac{\Delta_{K\pi}}{s}\left[1 + \frac{s\hat{\epsilon}_s}{M_\tau(m_s - m_u)}\right]\,. \tag{13}$$

Obtaining the three independent form factors ($F_0(s)$, $F_+(s)$ and $F_T(s)$) using as much experimental and theoretical knowledge as possible is the subject of the next section.

4. Hadronization of the scalar, vector and tensor currents

In this section we study the scalar, vector and tensor form factors. These are crucial in this work since they are needed SM inputs for binding the non-standard interactions. Therefore, it is fundamental to obtain them reliably (including associated errors) in order to have precise NP limits. We calculate the form factors using chiral perturbation theory, dispersion relations and lattice data. For the scalar and vector form factors this approach is discussed in refs. [19, 20, 55, 56]. We construct the tensor form factor following ref. [28] where an analogous work for the $\tau^- \to \pi^-\pi^0\nu_\tau$ channel was done. This tensor form factor is very special in this work. As we will see, it is connected with the A_{CP} observable that we introduced in section 1 and that we will study in much more detail in section 6.

We start our discussion with a brief reminder of the approach employed for the scalar form factor, $F_0(s)$. In a series of papers [56–60] an analysis for meson-meson scattering within Chiral Perturbation Theory with resonances for strangeness-changing coupled-channels was carried out and very precise information on the corresponding scalar form factors, light quark masses and related

chiral low-energy constants was obtained. We benefit from that analysis here [5]. In particular, we employ the update presented in Ref. [60] for the dispersive representation of the $K\pi$ channel, together with its corresponding uncertainties [6].

Now we turn to the vector form factor $F_+(s)$. In refs. [19, 20, 55], a dispersion relation for $F_+(s)$ was formulated and it was seen that a thrice-subtracted dispersion relation was optimal:

$$F_+(s) = \exp\left[\alpha_1 s + \frac{\alpha_2}{2}s^2 + \int_{s_{\pi K}}^{\infty} ds' \frac{\delta_1^{1/2}(s)}{(s')^3(s'-s-i\epsilon)}\right], \tag{14}$$

where α_1, α_2, and the one to set $F_+(0) = 1$ are the three subtraction constants, and $s_{\pi K} = (m_{\bar{K}^0} + m_{\pi^-})^2$. Eq. (14) shows that each additional subtraction in the dispersion relation gives rise to a further suppression factor $1/s'$ in the integrand, enhancing the relative importance of the low-energy input.

Finally, we study the hadronization of the tensor current, which was presented in equation (9). We will start with the calculation of this matrix element using Chiral Perturbation Theory. This will give us its normalization at zero-momentum transfer (equivalently, it will fix the first –and only in this case– subtraction constant). The energy dependence will be obtained solving numerically the dispersion relation, where the input phase corresponds to the one of the vector form factor in the elastic region [2].

The appropriate effective Lagrangian according to Ref. [62] is shown in the following equation,

$$\mathcal{L}_4 = \Lambda_1\langle t_+^{\mu\nu} f_{+\mu\nu}\rangle - i\Lambda_2\langle t_+^{\mu\nu} u_\mu u_\nu\rangle + \Lambda_3\langle t_+^{\mu\nu} t_{\mu\nu}^+\rangle + \Lambda_4\langle t_+^{\mu\nu}\rangle^2, \tag{15}$$

where $t_+^{\mu\nu} = u^\dagger t^{\mu\nu} u^\dagger + u t^{\mu\nu\dagger} u$, and $u_\mu = i[u^\dagger(\partial_\mu - ir_\mu)u - u(\partial_\mu - i\ell_\mu)u^\dagger]$. The non-linear representation of the pseudo-Goldstone bosons is $u = \exp\left(\frac{i}{\sqrt{2}F}\phi\right)$ where F is the pion decay constant in the chiral limit, and ℓ_μ and r_μ are left- and right-handed sources (also appearing in the operator with coefficient Λ_1 through $f_+^{\mu\nu} = uF_L^{\mu\nu}u^\dagger + u^\dagger F_R^{\mu\nu} u$ via the familiar field-strength tensors $F_{L,R}^{\mu\nu}$). The symbol $\langle ... \rangle$ denotes a trace in flavour space. The Λ_i are (real) low-energy constants which cannot be fixed by symmetries alone.

The explicit form of ϕ is given as follows:

$$\phi = \begin{pmatrix} \frac{\pi^0+\eta_q}{\sqrt{2}} & \pi^+ & K^+ \\ \pi^- & \frac{-\pi^0+\eta_q}{\sqrt{2}} & K^0 \\ K^- & \bar{K}^0 & \eta_s \end{pmatrix}, \tag{16}$$

where η_q and η_s are the non-strange and strange components of the $\eta - \eta'$ mesons (see e. g. eqs. (9) and (10) in ref. [63] and related discussion, we have used the excellent approximation $\pi^3 \sim \pi^0$ which comes from neglecting the isospin-suppressed mixing of the neutral pion with the $\eta - \eta'$ mesons [64]).

At the quark level (with corresponding field ψ), the tensor current has the form $\bar{\psi}\sigma_{\mu\nu}\bar{t}^{\mu\nu}\psi$,

[5] We thank Matthias Jamin for providing us with these data.

[6] For the analysis of the $K\pi$ spectra near threshold it is particularly important to employ a scalar form factor that is consistent with the information coming from S-wave $K\pi$ scattering (including the coupled channels $K\eta$ and $K\eta'$). The scalar form factor obtained in Ref. [60] is included in the RChL version of TAUOLA [61], but not in other releases.

where according to Ref. [62], the tensor source ($\bar{t}^{\mu\nu}$) is related to its chiral projections ($t^{\mu\nu}$ and $t^{\mu\nu\,\dagger}$) by means of

$$t^{\mu\nu} = P_L^{\mu\nu\lambda\rho}\bar{t}_{\lambda\rho}, \quad 4P_L^{\mu\nu\lambda\rho} = (g^{\mu\lambda}g^{\nu\rho} - g^{\mu\rho}g^{\nu\lambda} + i\epsilon^{\mu\nu\lambda\rho})\,. \tag{17}$$

Now let us compute the functional derivative of eq. (15) with respect to $\bar{t}_{\alpha\beta}$. The first thing to note is that only the operator with coefficient Λ_2 contributes to the decays we are analyzing,

$$\frac{\delta\mathcal{L}}{\delta\bar{t}_{\alpha\beta}} = -i\Lambda_2\frac{\delta}{\delta\bar{t}_{\alpha\beta}}\langle t_+^{\mu\nu}u_\mu u_\nu\rangle\,. \tag{18}$$

Putting the left and right sources to zero, expanding u in powers of ϕ and using the first of eqs. (17) we obtain,

$$\frac{\delta\mathcal{L}}{\delta\bar{t}_{\alpha\beta}} = \frac{-2i\Lambda_2}{F^2}\frac{\delta}{\delta\bar{t}_{\alpha\beta}}\left[\left(P_L^{\mu\nu\lambda\rho}\bar{t}_{\lambda\rho} + \bar{t}_{\lambda\rho}P_R^{\mu\nu\lambda\rho}\right)\partial_\mu\phi\partial_\nu\phi\right] = -\frac{i\Lambda_2}{F^2}[\partial^\alpha\phi, \partial^\beta\phi]\,. \tag{19}$$

In the calculation of the matrix element $i\langle\pi^0K^-|\frac{\partial\mathcal{L}}{\partial\bar{t}_{\alpha\beta}}|0\rangle$ we need the element $(1,3)$ of the previous matrix, which yields:

$$i\left\langle\pi^0K^-\middle|\frac{\delta\mathcal{L}}{\delta\bar{t}_{\alpha\beta}}\middle|0\right\rangle = \frac{\Lambda_2}{\sqrt{2}F^2}\left(p_K^\alpha p_0^\beta - p_0^\alpha p_K^\beta\right)\,. \tag{20}$$

From the same matrix element we obtain:

$$i\left\langle\pi^-\bar{K}^0\middle|\frac{\delta\mathcal{L}}{\delta\bar{t}_{\alpha\beta}}\middle|0\right\rangle = \frac{\Lambda_2}{F^2}\left(p_K^\alpha p_-^\beta - p_-^\alpha p_K^\beta\right)\,, \tag{21}$$

which checks explicitly the relative factor of $\frac{1}{\sqrt{2}}$ between the matrix elements for both decay channels.

As anticipated earlier, the value of Λ_2 is not restricted by symmetry requirements and cannot be fixed from phenomenology. Fortunately, the lattice QCD evaluation of Ref. [65] found $f_T^{\bar{K}^0\pi^-}(0) = 0.417(15)$. This, together with the fact that $F_T^{\bar{K}^0\pi^-}(0) = \frac{\Lambda_2}{F^2}$ implies that $\Lambda_2 = (11.1 \pm 0.4)$ MeV, that we will use in our numerical analysis. This value is consistent within one sigma with the one employed in Ref. [28] for the $\pi\pi$ channel.

Unlike the vector and scalar form factor cases, there is no experimental data that can help us constructing $F_T(s)$ so that we must rely only on theory. We calculate the energy-dependence of the tensor form factor $F_T(s)$ using again a phase dispersive representation as it is shown in refs. [2] and [28];

$$\frac{F_T(s)}{F_T(0)} = \exp\left[\frac{s}{\pi}\int_{s_{\pi K}}^{\infty} ds'\,\frac{\delta_T(s')}{s'(s'-s-i\epsilon)}\right]\,, \tag{22}$$

where $F_T^{\bar{K}^0\pi^-}(0) = \Lambda_2/F^2$ was calculated previously at leading order in the χPT framework (see eq. (21)), and $s_{\pi K} = (m_{\bar{K}^0} + m_{\pi^-})^2$. In this case it is clear, that lacking precise low-energy information, we cannot increase the number of subtractions of $F_T(s)$. This, in turn, implies a sizable sensitivity to the upper limit of the integral that is used numerically (s_{cut}), which is illustrated in our figure 1, where we consider the cases $s_{cut} = M_\tau^2, 4, 9$ GeV^2 [28] [7]. We take the differences between these

[7] In principle, one could try to reduce this sensitivity following the strategies employed in Ref. [66], but the procedure will again be limited in this case by the absence of measurements sensitive to $F_T(s)$.

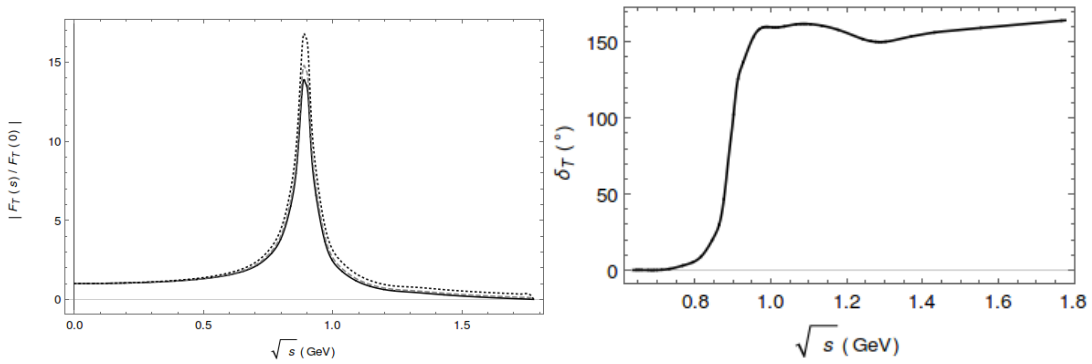

Figure 1: Modulus and phase, $|F_T(s)|$ (left) and $\delta_T(s) = \delta_+(s)$ (right), of the tensor form factor, $F_T(s)$. On the left plot, the dotted line corresponds to $s_{cut} = 9$ GeV^2, the dashed one to $s_{cut} = 4$ GeV^2, and the solid one to $s_{cut} = M_\tau^2$.

curves as an estimate of our systematic theoretical error on $F_T(s)/F_T(0)$. In the right panel of figure 1 we show the tensor form factor phase corresponding to $\delta_T(s) = \delta_+(s)$, with $\delta_+(s)$ from the fits in table 1 of Ref. [20]. In the inelastic region, our curve plotted for $\delta_T(s)$ lies within the error band shown in figure 2 of Ref. [2] [8]

5. Decay observables

In the rest frame of the τ lepton, the doubly differential decay width for the $\tau^- \to K_S\pi^-\nu_\tau$ process is

$$\frac{d^2\Gamma}{dsdt} = \frac{1}{32(2\pi)^3 M_\tau^3}\overline{|\mathcal{M}|^2}, \tag{23}$$

where $\overline{|\mathcal{M}|^2}$ will be calculated in what follows, s is the invariant mass of the $\pi^- K_S$ system taking values in the $(m_{K^0} + m_{\pi^-})^2 \leq s \leq M_\tau^2$ interval, and

$$t^\pm(s) = \frac{1}{2s}\left[2s(M_\tau^2 + m_{K^0}^2 - s) - \left(M_\tau^2 - s\right)\left(s + m_{\pi^-}^2 - m_{K^0}^2\right) \pm \left(M_\tau^2 - s\right)\sqrt{\lambda(s, m_{\pi^-}^2, m_{K^0}^2)}\right], \tag{24}$$

with $\lambda(x, y, z) = x^2 + y^2 + z^2 - 2xy - 2xz - 2yz$ being the usual Källen function and $t = (P_\tau - p_\pi)^2$.

5.1 Dalitz plots

By combining the equations of section 3, we obtain the following form for the amplitude (we will omit from now on the indices identifying the $K_S\pi^-$ charge channel)

$$\begin{aligned}\mathcal{M} =& \frac{G_F}{\sqrt{2}} V_{us}\sqrt{S_{EW}}(1 + \epsilon_L + \epsilon_R)\left[\left((p_K - p_\pi)^\mu + \frac{\Delta_{\pi K}}{s}(p_\pi + p_K)^\mu\right) L_\mu F_+(s)\right. \\ &+ \frac{\Delta_{K\pi}}{s}\left(1 + \frac{s\hat{\epsilon}_s}{M_\tau(m_s - m_u)}\right)(p_\pi + p_K)^\mu L_\mu F_0(s) \\ &\left. + 2i\hat{\epsilon}_T(p_K^\mu p_\pi^\nu - p_\pi^\mu p_K^\nu)L_{\mu\nu}F_T(s)\right].\end{aligned} \tag{25}$$

[8] Our phase is given in degrees while theirs is in radians.

The previous equation can be written as follows:

$$\mathcal{M} = \frac{G_F}{\sqrt{2}} V_{us} \sqrt{S_{EW}} (1 + \epsilon_L + \epsilon_R)(M_0 + M_+ + M_T), \tag{26}$$

where,

$$\begin{aligned} M_+ &= \left((p_K - p_\pi)^\mu + \frac{\Delta_{\pi K}}{s} (p_\pi + p_K)^\mu \right) L_\mu F_+(s), \\ M_0 &= \frac{\Delta_{K\pi}}{s} \left(1 + \frac{s\hat{\epsilon}_s}{M_\tau (m_s - m_u)} \right) (p_\pi + p_K)^\mu L_\mu F_0(s), \\ M_T &= 2i\hat{\epsilon}_T (p_K^\mu p_\pi^\nu - p_\pi^\mu p_K^\nu) L_{\mu\nu} F_T(s). \end{aligned} \tag{27}$$

The squared of the amplitude, computed from eq. (26), has six (all non-vanishing) contributions: three of them coming from scalar-scalar (M_{00}), vector-vector (M_{++}), and tensor-tensor (M_{TT}) contributions, and the remaining three from interference terms (M_{0+}, M_{0T}, and M_{+T}). Their expressions are

$$\begin{aligned} M_{0+} =& \Big[-2M_\tau^2 Re[F_+(s)F_0^*(s)]\Delta_{K\pi} \left(1 + \frac{s\hat{\epsilon}_s}{M_\tau(m_s - m_u)} \right) \\ & \times \left(s(M_\tau^2 - s + \Sigma_{K\pi} - 2t) + M_\tau^2 \Delta_{K\pi} \right) \Big], \end{aligned} \tag{28}$$

$$M_{T+} = -4\hat{\epsilon}_T M_\tau^3 s Re[F_T(s)F_+^*(s)] \left(1 - \frac{s}{M_\tau^2} \right) \lambda(s, m_\pi^2, m_K^2), \tag{29}$$

$$\begin{aligned} M_{T0} =& 4\Delta_{K\pi}\hat{\epsilon}_T M_\tau s Re[F_T(s)F_0^*(s)] \left(1 + \frac{s\epsilon_s}{M_\tau(m_s - m_u)} \right) \\ & \times \left[s(M_\tau^2 - s + \Sigma_{K\pi} - 2t) + M_\tau^2 \Delta_{K\pi} \right], \end{aligned} \tag{30}$$

$$M_{00} = (\Delta_{K\pi})^2 M_\tau^4 \left(1 - \frac{s}{M_\tau^2} \right) |F_0(s)|^2 \left(1 + \frac{s\hat{\epsilon}_s}{M_\tau(m_s - m_u)} \right)^2, \tag{31}$$

$$\begin{aligned} M_{++} =& |F_+(s)|^2 \Big[M_\tau^4 (s + \Delta_{K\pi})^2 - M_\tau^2 s \Big(2\Delta_{K\pi}(-m_K^2 + s + 2t - m_\pi^2) \\ & - \Delta_{K\pi}^2 + s(s + 4t) \Big) + 4m_K^2 s^2 (m_\pi^2 - t) + 4s^2 t(s + t - m_\pi^2) \Big], \end{aligned} \tag{32}$$

$$\begin{aligned} M_{TT} =& 4\hat{\epsilon}_T^2 F_T^2 s^2 \Big[m_\pi^4 (M_\tau^2 - s) - 2m_\pi^2 (M_\tau^2 - s)(s + 2t - m_K^2) - m_K^4 (3M_\tau^2 + s) \\ & + 2m_K^2 \left((s + M_\tau^2)(s + 2t) - 2M_\tau^4 \right) - s \left((s + 2t)^2 - M_\tau^2 (s + 4t) \right) \Big], \end{aligned} \tag{33}$$

where we have introduced $\Sigma_{K\pi} = m_\pi^2 + m_K^2$.

Taking into account all previous contributions we can finally write the unpolarized spin-averaged squared amplitude as follows

$$\overline{|\mathcal{M}|^2} = G_F^2 |V_{us}|^2 S_{EW} (1 + \epsilon_L + \epsilon_R)^2 (M_{0+} + M_{T+} + M_{T0} + M_{00} + M_{++} + M_{TT}). \tag{34}$$

It is convenient in the study of the Dalitz plots to define the following observable introduced in Ref. [28]

$$\tilde{\Delta}(\hat{\epsilon}_S, \hat{\epsilon}_T) = \frac{\left| \overline{|\mathcal{M}(\hat{\epsilon}_S, \hat{\epsilon}_T)|^2} - \overline{|\mathcal{M}(0,0)|^2} \right|}{\overline{|\mathcal{M}(0,0)|^2}}, \tag{35}$$

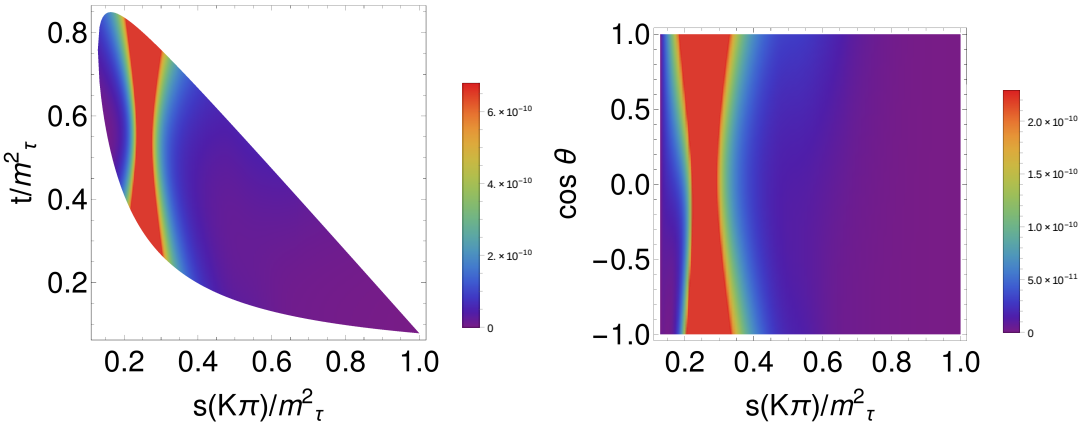

Figure 2: Dalitz plot distribution $\overline{|\mathcal{M}|^2}_{00}$ in the SM, eq. (34): Differential decay distribution for $\tau^- \to K_S\pi^-\nu_\tau$ in the (s,t) variables (left). The right-hand figure shows the differential decay distribution in the $(s,\cos\theta)$ variables, eq. (36). The Mandelstam variables, s and t, are normalized to M_τ^2.

which is sensitive to the relative difference between the squared matrix element in presence/absence of NP contributions (the SM case corresponds to $\mathcal{M}(0,0)$).

In the left panel of figure 2 we show the Dalitz plot for the SM case in the (s,t) variables, and in the left part of figures 3 and 4 we show the corresponding plots for the values $(\hat{\epsilon}_S = -0.5, \hat{\epsilon}_T = 0)$ and $(\hat{\epsilon}_S = 0, \hat{\epsilon}_T = 0.6)$, respectively. The election of these particular values of the $\hat{\epsilon}_{S,T}$ is discussed in section 5.5.

The important thing to note from the SM result in figure 2 is that the dynamics is dominated by the $K^*(892)$ vector resonance.

The left panel of figures 3 and 4 shows the relative modification of the squared matrix element for non-zero reasonable values of $\hat{\epsilon}_S$ and $\hat{\epsilon}_T$ in the (s,t) plane. Although large variations are seen in a couple of regions close to the border of the Dalitz plot in figure 3 (left), these correspond to zones with very suppressed probability, as can be seen in figure 2 (left). On the contrary, the regions with larger probability have a small relative change, according to figure 3 (left). In figure 4 (left) the region with the most noticeable change (though still smaller than those seen in figure 3) is located very close to the s minimum of the Dalitz plot, which has very small probability density in figure 2 (left). This region quite overlaps with one of the two mentioned for the fig. 3 left plot. Because of this feature, observing a deviation from the SM result in this region could be due to both tensor and non-standard scalar interactions. On the contrary, a deviation in the region of small t values would be signalling spin-zero NP contribution. In any case, changes are very small in the region most densely populated by measured events in both left plots of figs. 3 and 4. Due to this, we conclude that it will be extremely challenging to identify NP contributions in the (s,t) Dalitz plot even with the large data samples accumulated by the end of operation of Belle-II [67].

5.2 Angular distribution

In this section we are going to study the angular dependence of the decay distribution. It is convenient to work in the rest frame of the hadronic system, in which we have $\vec{p}_\pi + \vec{p}_K = \vec{p}_\tau - \vec{p}_\nu = \vec{0}$,

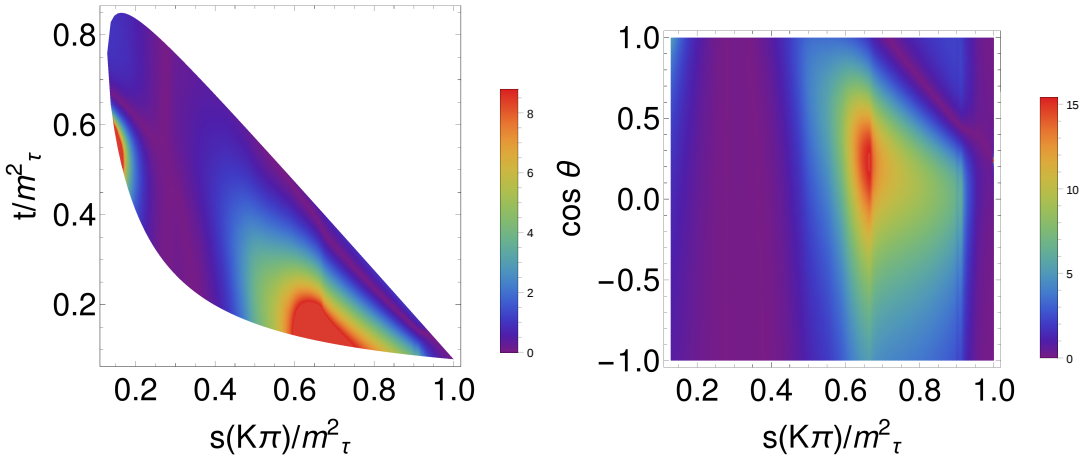

Figure 3: Dalitz plot distribution $\tilde{\Delta}(\hat{\epsilon}_S, \hat{\epsilon}_T)$, eq. (35), in the $\tau^- \to K_S\pi^-\nu_\tau$ decays: left-hand side corresponds to eq. (34) and the right-hand side corresponds to the differential decay distribution in the $(s, \cos\theta)$ variables, eq. (36), both with $(\hat{\epsilon}_S = -0.5, \hat{\epsilon}_T = 0)$. The Mandelstam variables, s and t, are normalized to M_τ^2.

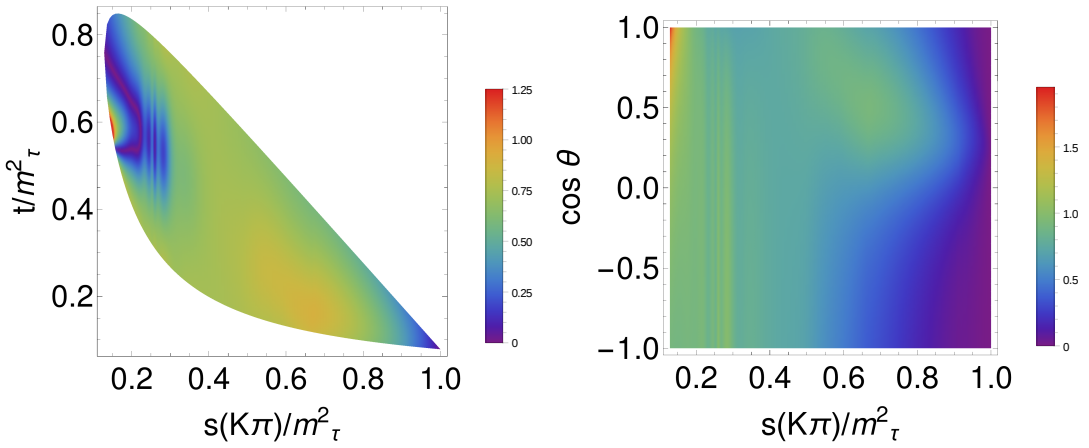

Figure 4: Dalitz plot distribution $\tilde{\Delta}(\hat{\epsilon}_S, \hat{\epsilon}_T)$, eq. (35), in the $\tau^- \to K_S\pi^-\nu_\tau$ decays: left-hand side corresponds to eq. (34) and the right-hand side corresponds to the differential decay distribution in the $(s, \cos\theta)$ variables, eq. (36), both with $(\hat{\epsilon}_S = 0, \hat{\epsilon}_T = 0.6)$. The Mandelstam variables, s and t, are normalized to M_τ^2.

consequently the tau lepton and the pion energies are given by $E_\tau = (s + M_\tau^2)/(2\sqrt{s})$ and $E_\pi = (s + m_\pi^2 - m_K^2)/(2\sqrt{s})$.

We will study the decay distribution in terms of the $(s, \cos\theta)$ variables, where θ is the angle between the three-momenta of the pion and the three-momenta of the tau lepton, this angle is related to the invariant t variable by $t = M_\tau^2 + m_\pi^2 - 2E_\tau E_\pi + 2|\vec{p}_\pi||\vec{p}_\tau|\cos\theta$, where $|\vec{p}_\pi| = \sqrt{E_\pi^2 - m_\pi^2}$ and $|\vec{p}_\tau| = \sqrt{E_\tau^2 - M_\tau^2}$ [9].

Changing variables to $(s, \cos\theta)$ in eq. (23) we obtain the following:

[9]The tau lifetime and decay width (τ_τ and Γ_τ, respectively) are defined in the τ rest frame. Consequently, their values are boosted in the reference frame considered in this subsection.

$$\frac{d^2\Gamma}{d\sqrt{s}d\cos\theta} = \frac{G_F^2|V_{us}|^2 S_{EW}}{128\pi^3 M_\tau}(1+\epsilon_L+\epsilon_R)^2\left(\frac{M_\tau^2}{s}-1\right)^2 |\vec{p}_{\pi^-}|\Bigg\{\Delta_{\pi K}^2|F_0(s)|^2$$

$$\times\left(1+\frac{s\hat{\epsilon}_S}{M_\tau(m_s-m_u)}\right)^2 + 16|\vec{p}_{\pi^-}|^2 s^2\left|-\frac{F_+(s)}{2M_\tau}+\hat{\epsilon}_T F_T(s)\right|^2$$

$$+4|\vec{p}_{\pi^-}|^2 s\left(1-\frac{s}{M_\tau^2}\right)\cos^2\theta\left[|F_+(s)|^2 - 4s\hat{\epsilon}_T^2|F_T(s)|^2\right] + 4\Delta_{\pi K}|\vec{p}_{\pi^-}|\sqrt{s}\cos\theta$$

$$\times\left(1+\frac{s\hat{\epsilon}_S}{M_\tau(m_s-m_u)}\right)\left[-Re\left[F_0(s)F_+^*(s)\right]+\frac{2s\hat{\epsilon}_T}{M_\tau}Re\left[F_T(s)F_0^*(s)\right]\right]\Bigg\}. \tag{36}$$

The Dalitz plots for the $(s,\cos\theta)$ variables are shown on the right panels of figures 2, 3 and 4 (in these last two the observable $\tilde{\Delta}(\hat{\epsilon}_S,\hat{\epsilon}_T)$ is plotted). On figure 2 we plot the SM case, and in figures 3 and 4 we show Dalitz plots for the values $(\hat{\epsilon}_S=-0.5,\ \hat{\epsilon}_T=0)$ and $(\hat{\epsilon}_S=0,\ \hat{\epsilon}_T=0.6)$, respectively. The SM plot gives equivalent information in the $(s,\cos\theta)$ variables as the one seen in the (s,t) variables (right versus left plot of figure 2). Comparing both panels of figs. 3 one can see that one of the enhanced regions in the (s,t) plot (the one at very low s values) is washed away in the $(s,\cos\theta)$ diagram, while the other is slightly further enhanced in a limited region $(0\leq\cos\theta\leq 0.5)$. The comparison of the left and right plots of figure 4 shows that the enhanced area for large t values is a bit more prominent in the $(s,\cos\theta)$ distribution (for nearly maximal $\cos\theta$) although again it will be very hard to disentangle these possible deviations from the SM patterns in near future data.
Assuming approximate lepton universality, using the bounds from Ref. [36] (obtained analyzing Kaon (semi)leptonic decays) $\hat{\epsilon}_S\sim -8\times10^{-4}$, $\hat{\epsilon}_T\sim 6\times10^{-3}$ (maximum allowed absolute values at one standard deviation) minimizes the deviations from the SM to unobservable level both in the (s,t) and $(s,\cos\theta)$ Dalitz plots.

5.3 Decay rate

Integrating eq. (23) upon the t variable we obtain the invariant mass distribution as follows

$$\begin{aligned}\frac{d\Gamma}{ds} =& \frac{G_F^2|V_{us}|^2 M_\tau^3 S_{EW}}{384\pi^3 s}(1+\epsilon_L+\epsilon_R)^2\left(1-\frac{s}{M_\tau^2}\right)^2\lambda^{1/2}(s,m_\pi^2,m_K^2)\\ &\times[X_{VA}+\hat{\epsilon}_S X_S+\hat{\epsilon}_T X_T+\hat{\epsilon}_S^2 X_{S^2}+\hat{\epsilon}_T^2 X_{T^2}],\end{aligned} \tag{37}$$

where

$$X_{VA} = \frac{1}{2s^2}\left[3|F_0(s)|^2\Delta_{K\pi}^2 + |F_+(s)|^2\left(1+\frac{2s}{M_\tau^2}\right)\lambda(s,m_\pi^2,m_K^2)\right], \tag{38a}$$

$$X_S = \frac{3}{sM_\tau}|F_0(s)|^2\frac{\Delta_{K\pi}^2}{m_s-m_d}, \tag{38b}$$

$$X_T = \frac{6}{sM_\tau}Re[F_T(s)F_+^*(s)]\lambda(s,m_\pi^2,m_K^2), \tag{38c}$$

$$X_{S^2} = \frac{3}{2M_\tau^2}|F_0(s)|^2\frac{\Delta_{K\pi}^2}{(m_s-m_u)^2}, \tag{38d}$$

$$X_{T^2} = \frac{4}{s}|F_T(s)|^2\left(1+\frac{s}{2M_\tau^2}\right)\lambda(s,m_\pi^2,m_K^2). \tag{38e}$$

Note from the previous equations that the only possible source of CP violation coming from the hadronic part is due to the Vector-Tensor interference, we will comment about this in section 6.

In figure 5, we plot the invariant mass distribution of the $K\pi$ system for $\tau^- \to K_S\pi^-\nu_\tau$ decays for the SM case and for ($\hat{\epsilon}_S = -0.5$, $\hat{\epsilon}_T = 0$) and ($\hat{\epsilon}_S = 0$, $\hat{\epsilon}_T = 0.6$) which would be realistic values for these couplings, according to their impact on the decay width. Despite the logarithmic scale of the plot, the deviations from the SM curve shown in figure 5 are too large when they are confronted with the Belle measurements of this spectrum, as we will see in the fits of section 5.5. This will allow us to set better bounds on $\hat{\epsilon}_{S,T}$ than those used in this subsection.

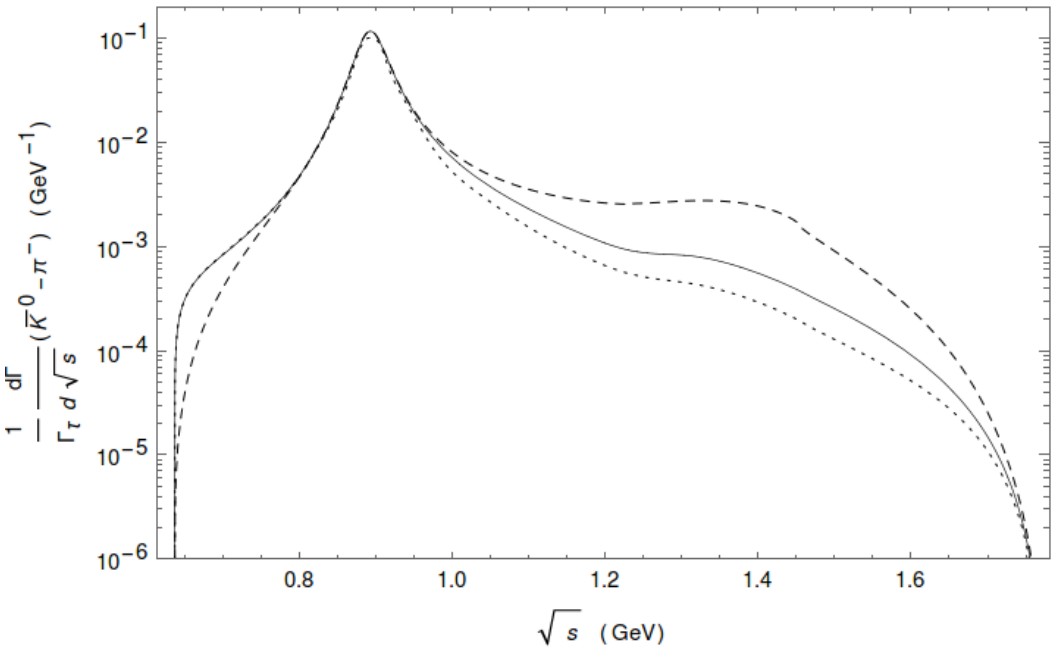

Figure 5: The $\bar{K}^0\pi^-$ hadronic invariant mass distribution for the SM (solid line) and $\hat{\epsilon}_S = -0.5$, $\hat{\epsilon}_T = 0$ (dashed line) and $\hat{\epsilon}_S = 0$, $\hat{\epsilon}_T = 0.6$ (dotted line). The decay distributions are normalized to the tau decay width.

5.4 Forward-backward asymmetry

Now we turn to the study of the forward-backward asymmetry, which is defined in the following way

$$\mathcal{A}_{K\pi}(s) = \frac{\int_0^1 d\cos\theta \frac{d^2\Gamma}{ds d\cos\theta} - \int_{-1}^0 d\cos\theta \frac{d^2\Gamma}{ds d\cos\theta}}{\int_0^1 d\cos\theta \frac{d^2\Gamma}{ds d\cos\theta} + \int_{-1}^0 d\cos\theta \frac{d^2\Gamma}{ds d\cos\theta}} \,. \tag{39}$$

We find the analytical expression for this observable substituting eq. (36) into eq. (39) and integrating upon the $\cos\theta$ variable with the following result [10]

$$\begin{aligned}\mathcal{A}_{K\pi} =& \frac{3\sqrt{\lambda(s, m_\pi^2, m_K^2)}}{2s^2[X_{VA} + \hat{\epsilon}_S X_S + \hat{\epsilon}_T X_T + \hat{\epsilon}_S^2 X_{S^2} + \hat{\epsilon}_T^2 X_{T^2}]} \left(1 + \frac{s\hat{\epsilon}_S}{M_\tau(m_s - m_u)}\right) \Delta_{\pi K} \\ & \times \left[-Re[F_0(s)F_+^*(s)] + \frac{2s\hat{\epsilon}_T}{M_\tau} Re[F_T(s)F_0^*(s)]\right] .\end{aligned} \tag{40}$$

Before studying the forward-backward asymmetry in the general case, it is important to study its behaviour in the standard model case. If we set $\epsilon_R = \epsilon_L = \hat{\epsilon}_S = \hat{\epsilon}_T = 0$ we get the SM forward-backward asymmetry, which is plotted in the solid line of figure 6.

The important thing to note from the SM result in figure 6 (solid line) is that the graph is peaked around $\sqrt{s} \sim 0.6$ GeV so that this is an important region to analyze and pay special attention. It was already emphasized long ago that a measurement of the forward-backward asymmetry in this decay channel would be crucial in improving our knowledge of both vector and scalar form factors [68] [11].

For the more general case where we include NP interactions, we have figure 6 (dashed and dotted lines), where we plot $\mathcal{A}_{K\pi}$ for the values ($\hat{\epsilon}_S = -0.5$, $\hat{\epsilon}_T = 0$) and ($\hat{\epsilon}_S = 0$, $\hat{\epsilon}_T = 0.6$) [12], and we compare those plots with the SM case. There we can see that for quite large $\hat{\epsilon}_T$ values some difference is appreciated for the tensor case; otherwise it may not be possible to disentangle it from the standard contribution. Conversely, for non-standard scalar interactions the changes are more noticeable since $A_{K\pi}$ flips sign with respect to the SM. Note also that for scalar interactions the value of $A_{K\pi}$ gets smaller in magnitude as s increases. If it is possible to measure $A_{K\pi}$ in a low-energy bin, this would ease the identification of this type of NP in $A_{K\pi}$.

If we make the comparison with more realistic limits for the NP values [36] (under the assumption of approximate lepton universality), it is impossible to identify any departures from the SM prediction in this observable. For this reason, we make use of the following convenient definition introduced in Ref. [28]

$$\Delta\mathcal{A}_{K\pi} \;=\; \mathcal{A}_{K\pi}(s, \hat{\epsilon}_S, \hat{\epsilon}_T) - \mathcal{A}_{K\pi}(s, 0, 0)\,. \tag{41}$$

The corresponding (unmeasurably small) deviations from the SM result are plotted in figure 7.

[10] In eq. (40) we use $\mathcal{A}_{K\pi}$ to emphasize the decay channel under consideration to distinguish it to the other two-meson decay modes. Otherwise we will also be using the most common notation A_{FB} for this observable.

[11] We note that in this reference, and also later on in Refs. [22, 69], the angle θ used to compute A_{FB} is defined between the three-momenta of the tau lepton and the K_S in the di-meson rest frame. Taking into account the different sign conventions, it can be checked there is reasonable agreement with these works in the elastic region.

[12] Again, as we mentioned when we discussed the Dalitz plots, we will justify the use of these particular values in the next section.

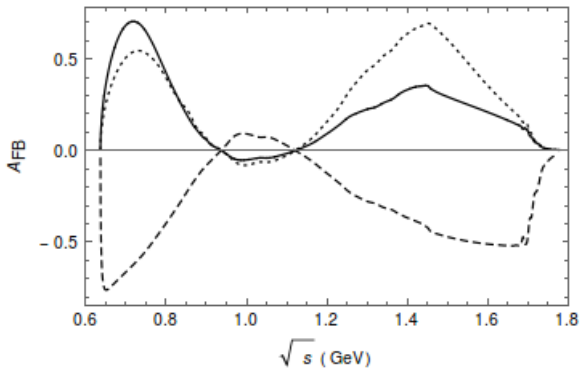

Figure 6: Forward-backward asymmetry in $\tau^- \to K_S\pi^-\nu_\tau$ decays compared with the SM prediction (solid line). The dashed line corresponds to $\hat{\epsilon}_S = -0.5$, $\hat{\epsilon}_T = 0$, and the dotted line corresponds to $\hat{\epsilon}_S = 0$, $\hat{\epsilon}_T = 0.6$.

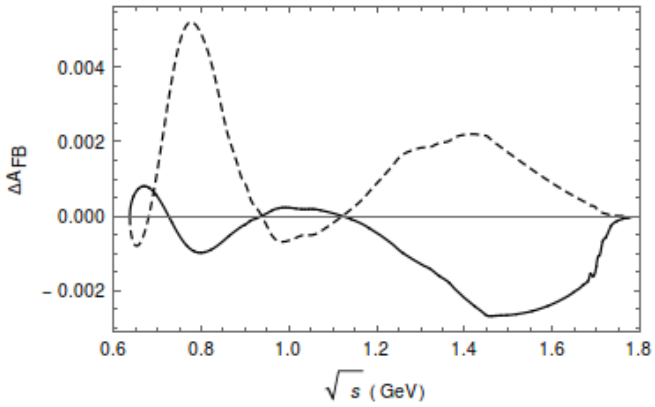

Figure 7: Deviations from the SM forward-backward asymmetry, $\Delta\mathcal{A}_{K\pi}$, in $\tau^- \to K_S\pi^-\nu_\tau$ decays using the bounds from Ref. [36]. The solid line corresponds to $\hat{\epsilon}_S = -8 \times 10^{-4}$, $\hat{\epsilon}_T = 0$ and the dashed line to $\hat{\epsilon}_S = 0$, $\hat{\epsilon}_T = 6 \times 10^{-3}$.

5.5 Limits on $\hat{\epsilon}_S$ and $\hat{\epsilon}_T$

Our purpose in this section is to set bounds on the effective couplings $\hat{\epsilon}_S$ and $\hat{\epsilon}_T$. We achieve this by comparing the total width Γ (which depends explicitly on the NP couplings $\hat{\epsilon}_S$ and $\hat{\epsilon}_T$) with the SM width Γ^0 (obtained by neglecting NP interactions which we get by setting $\hat{\epsilon}_S = \hat{\epsilon}_T = 0$). This comparison is conveniently implemented with the introduction of the observable Δ which we define as follows

$$\Delta \equiv \frac{\Gamma - \Gamma^0}{\Gamma^0} = \alpha\hat{\epsilon}_S + \beta\hat{\epsilon}_T + \gamma\hat{\epsilon}_S^2 + \delta\hat{\epsilon}_T^2, \tag{42}$$

where we obtained the following results for the coefficients: $\alpha \in [0.30, 0.34]$, $\beta \in [-2.92, -2.35]$, $\gamma \in [0.95, 1.13]$ and $\delta \in [3.57, 5.45]$.

With the help of the Δ observable we obtain our limits for the $\hat{\epsilon}_S$ and $\hat{\epsilon}_T$ couplings in two different ways. First, we set one of the couplings to zero and obtain bounds for the other, and viceversa. This process gives us the two parabolas shown in figure 8.

The second way in which we set constraints is again using Eq. (42), but now taking the general case where both couplings are non-vanishing. In this case we obtain the ellipse shown in figure 9.

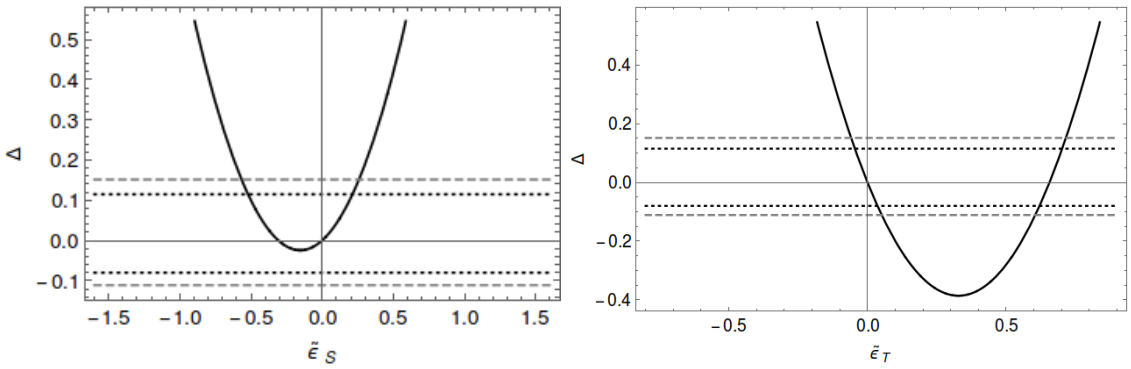

Figure 8: Δ as a function of $\hat{\epsilon}_S$ for $\hat{\epsilon}_T = 0$ (left hand) and of $\hat{\epsilon}_T$ for $\hat{\epsilon}_S = 0$ (right hand) for $\tau^- \to K_S\pi^-\nu_\tau$ decays. Horizontal lines represent the values of Δ according to the current measurement and theory errors (at three standard deviations) of the branching ratio (dashed line) and in the hypothetical case where the measured branching ratio at Belle-II has a three times reduced uncertainty (dotted line).

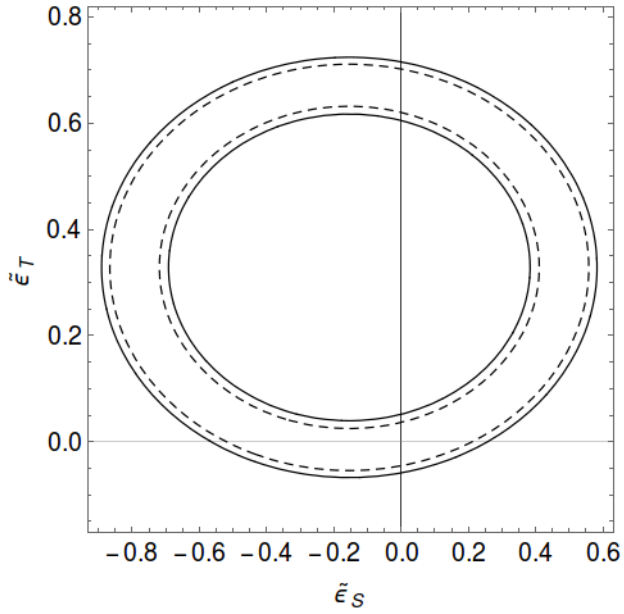

Figure 9: Constraints on the scalar and tensor couplings obtained from $\Delta(\tau^- \to K_S\pi^-\nu_\tau)$ using theory and the measured value reported in the PDG, with their corresponding uncertainties at three standard deviations (solid line). The dashed line ellipse corresponds to the case where the measurements error was reduced to a third of the current uncertainty.

For the convenience of the reader we summarize our findings for the constraints in the following table.

Next we will consider fits to the branching ratio and decay spectrum [13] of the $\tau^- \to K_S\pi^-\nu_\tau$ decays as measured by Belle [16]. We will pay special attention to the possible explanation of the conflicting data points (bins 5, 6 and 7) by the non-standard interactions. Therefore, we will

[13] We thank Denis Epifanov for providing us with these data.

Δ limits	$\hat{\epsilon}_S(\hat{\epsilon}_T = 0)$	$\hat{\epsilon}_T(\hat{\epsilon}_S = 0)$	$\hat{\epsilon}_S$	$\hat{\epsilon}_T$
Current bounds	$[-0.57, 0.27]$	$[-0.059, 0.052] \cup [0.60, 0.72]$	$[-0.89, 0.58]$	$[-0.07, 0.72]$
Future bounds	$[-0.52, 0.22]$	$[-0.047, 0.036] \cup [0.62, 0.71]$	$[-0.87, 0.56]$	$[-0.06, 0.71]$

Table 1: Constraints on the scalar and tensor couplings obtained through the limits on the current branching ratio at three standard deviations using the current theory and experimental errors and assuming the latter be reduced to a third ('Future bounds'). This last case should be taken only as illustrative of the improvement that can be achieved thanks to higher-statistics measurements, even in absence of any progress on the theory side. It is clear that the knowledge of $\hat{\epsilon}_{S,T}$ using $\tau^- \to K_S\pi^-\nu_\tau$ decays data is limited by theory uncertainties.

consider fits with and without these data points. In all our fits, as explained e. g. in Ref. [55], we will not consider the first data point (as it lies below the threshold for physical K_S and π^- masses) and will disregard the data from the last 10 bins, as suggested by the Belle collaboration.
The χ^2 function minimized in our fits is

$$\sum_i \left(\frac{N_i^{exp} - N_i^{th}}{\sigma_{N_i}} \right)^2 + \left(\frac{BR^{exp} - BR^{th}}{\sigma_{BR}^{exp}} \right)^2 , \tag{43}$$

where the sum over the i bins may or may not include the $i = 5, 6, 7$ bins. We will consider the measurement of BR^{exp} reported in the Belle paper [16] (and not the PDG [9] or the HFLAV [70] values), as discussed in Ref. [55]. Along our fits we float the meson form factors within their estimated uncertainty bands and our quoted results take these errors into account. We present our results in table 2.

Best fit values	$\hat{\epsilon}_S$	$\hat{\epsilon}_T$	χ^2	χ^2 in the SM
Excluding $i = 5, 6, 7$ bins	$(1.3 \pm 0.9) \times 10^{-2}$	$(0.7 \pm 1.0) \times 10^{-2}$	$[72, 73]$	$[74, 77]$
Including $i = 5, 6, 7$ bins	$(0.9 \pm 1.0) \times 10^{-2}$	$(1.7 \pm 1.7) \times 10^{-2}$	$[83, 86]$	$[91, 95]$

Table 2: Best fit values to the Belle spectrum and branching ratio of the $\tau^- \to K_S\pi^-\nu_\tau$ decays [16]. The cases where the $i = 5, 6, 7$ bins are excluded/included are considered. We display the reference results obtained floating $\hat{\epsilon}_S$ and $\hat{\epsilon}_T$ simultaneously. In the last two columns the χ^2 of these fits is compared to the SM result.

6. CP violation

The observable A_{CP}, measured by BaBar [6] has the right magnitude but the wrong sign compared with the SM prediction (tiny corrections from direct CP violation are neglected along this section). It is defined as

$$A_{CP} = \frac{\Gamma(\tau^+ \to \pi^+ K_S \bar{\nu}_\tau) - \Gamma(\tau^- \to \pi^- K_S \nu_\tau)}{\Gamma(\tau^+ \to \pi^+ K_S \bar{\nu}_\tau) + \Gamma(\tau^- \to \pi^- K_S \nu_\tau)} . \tag{44}$$

In the SM, A_{CP} is given by the neutral kaon mixing contribution. Thus, it comes from the analogous asymmetry measured in semileptonic kaon decays [2] ($\ell = e, \mu$)

$$\frac{\Gamma(K_L \to \pi^- \ell^+ \nu_\ell) - \Gamma(K_L \to \pi^+ \ell^- \bar{\nu}_\ell)}{\Gamma(K_L \to \pi^- \ell^+ \nu_\ell) + \Gamma(K_L \to \pi^+ \ell^- \bar{\nu}_\ell)} = 3.32(6) \times 10^{-3} , \tag{45}$$

up to small corrections caused by the fact that the K_S is reconstructed at the B-factories through its $\pi^+\pi^-$ decay mode with a decay time of the order of the K_S lifetime. This changes the previous value to $A_{CP}^{SM} = 3.6(1) \times 10^{-3}$ [10], that is 2.8 σ away from the BaBar measurement, $A_{CP} = -3.6(2.3)(1.1) \times 10^{-3}$.

Ref. [3] shows that beyond the SM (BSM) interactions modify A_{CP} to

$$A_{CP} = \frac{A_{CP}^{SM} + A_{CP}^{BSM}}{1 + A_{CP}^{SM} \times A_{CP}^{BSM}}, \tag{46}$$

where [2] [14]

$$A_{CP}^{BSM} = \frac{2\sin\delta_T^W |\hat{\epsilon}_T| G_F^2 |V_{us}|^2 S_{EW}}{256\pi^3 M_\tau^2 \Gamma(\tau \to K_S \pi \nu_\tau)} \int_{s_{\pi K}}^{M_\tau^2} \mathrm{d}s |f_+(s)||F_T(s)| \sin(\delta_+(s) - \delta_T(s)) \frac{\lambda^{3/2}(s, m_\pi^2, m_K^2)(M_\tau^2 - s)^2}{s^2}, \tag{47}$$

where δ_T^W corresponds to the relative weak phase between the SM (V-A) and the tensor contributions. Ref. [2] uses $SU(2)_L$ invariance of the weak interactions within the EFT to find stringent constraints on $\Im m[\hat{\epsilon}_T]$, using the $D-\bar{D}$ mixing measurements and the upper limit on the electric dipole moment of the neutron. This yields the bound $2\Im m[\hat{\epsilon}_T] < 10^{-5}$, that we will use. To see that δ_T^W is a small parameter, we remind the limits from the global EFT analysis of NP in Kaon (semi)leptonic decays [36], according to which $|\epsilon_T| = (0.5 \pm 5.2) \times 10^{-3}$. Considering this, $\sin\delta_T^W |\hat{\epsilon}_T| \sim \Im m[\hat{\epsilon}_T]$ and the numerical evaluation of eq. (47) is straightforward with the inputs at hand.

We have computed eq. (47) using $|F_T(s)|$ obtained with $s_{cut} = M_\tau^2, 4, 9$ GeV^2 (shown in the left panel of fig. 1) and with $\delta_T(s)$ varying (smoothly) within the band shown in fig. 2 of Ref. [2], as we agree with the estimation of this uncertainty [15]. The errors on $|F_+(s)|$ and $\delta_+(s)$ are negligible compared to the uncertainties on $F_T(s)$. Among these two uncertainties, the error on $\delta_T(s)$ dominates: changing s_{cut} for a given $\delta_T(s)$ can modify A_{CP}^{BSM} by a factor three, at most; while, with a fixed s_{cut}, A_{CP}^{BSM} can be vanishing for $\delta_T(s) \to \delta_+(s)$ also in the inelastic region. In this way, we find

$$A_{CP}^{BSM} < 8 \cdot 10^{-7}, \tag{48}$$

which is a slightly weaker bound than the one reported in Ref. [2]: $A_{CP}^{BSM} < 3 \cdot 10^{-7}$. This small difference comes mainly from our accounting for the variation in s_{cut} and also for the slightly different phase $\delta_+(s)$ in both analyses. In any case, it is clear that heavy BSM interactions can only modify A_{CP} at the 10^{-6} level at most, which is at least three orders of magnitude smaller than the theoretical uncertainty in its prediction (which is, in turn, some 25 times smaller than the error of the BaBar measurement). Therefore, any conclusive anomaly in A_{CP} must be explained outside the framework considered in this paper (and in Ref. [2]); for instance, by BSM effects of very light particles.

7. Conclusions

In this work we focused in the study of the $\tau^- \to (K\pi)^-\nu_\tau$ decays. Here we have studied the effect of NP in several interesting observables like Dalitz plots, decay spectrum and forward-

[14] We remind that c_T in this reference equals $2\hat{\epsilon}_T$ in our notation.

[15] See also Ref. [71], where NP bounds obtained from $\tau^- \to K^-\nu_\tau$ decays are first discussed.

backward asymmetry. The effect of this NP was encoded in the effective couplings $\hat{\epsilon}_S$ and $\hat{\epsilon}_T$ for which we have also set constraints. All these observables were calculated in the SM case as well, in order to be able to compare the way in which NP could manifest. Apart from that, we have three main conclusions for this work:

- In agreement with Ref. [2], we confirm that it is not possible to understand within the low-energy limit of the SMEFT framework the BaBar measurement [6] of the CP asymmetry, which disagrees at 2.8σ with the SM prediction [10]. As a consequence of our dedicated treatment of the uncertainties on the tensor form factor, we find an slightly weaker bound than in Ref. [2], $A_{CP}^{BSM} \leq 8 \cdot 10^{-7}$, which is anyway some three (five) orders of magnitude smaller than the theoretical uncertainty in its prediction (the error of the BaBar measurement). If the BaBar anomaly is confirmed, its explanation must be due to light NP. A determination of this quantity with Belle-I data, together with the future measurement at Belle-II [67], will shed light on this puzzle.

- The bins number 5, 6 and 7 of the Belle measurement [16] of the $K_S\pi^-$ mass spectrum in $\tau^- \to K_S\pi^-\nu_\tau$ decays could not find an explanation using a scalar form factor obtained from the corresponding partial-wave of a meson-meson scattering coupled channels analysis [18, 57] [16]. We have shown here, for the first time, that non-standard scalar or tensor interactions produced by heavy NP are not capable of explaining these data points either. Again a caveat remains with respect to light NP effects, which are beyond the scope of this work.

- Current branching ratio and spectrum measurements of the $\tau^- \to K_S\pi^-\nu_\tau$ decays restrict the NP effective couplings, $\hat{\epsilon}_S$ and $\hat{\epsilon}_T$, as we have studied in this work for the first time. Our results are consistent with naive expectations: while the considered decays set bounds similar to those coming from hyperon semileptonic decays (which are at the level of a few TeV NP energy scale under reasonable assumptions), they are not competitive with (semi)leptonic Kaon decays, that could probe NP at a scale of order $O(500)$ TeV for the case of scalar interactions. However, we must say that tensor interactions in $\tau^- \to (K\pi)^-\nu_\tau$ decays are probed with similar NP energy reach than in (semi)leptonic Kaon and hyperon decays. Therefore, the corresponding comparisons for $\hat{\epsilon}_T$ are meaningful tests of lepton universality and under this assumption tau decays can complement Kaon and hyperon physics in restricting tensor interactions.

Recently, several new works have addressed the same process that we have analyzed following the LEFT, see for example refs. [72–74].

References

[1] J. Rendón, P. Roig and G. Toledo Sánchez, Phys. Rev. D **99**, no.9, 093005 (2019).

[16] The effect of the otherwise dominant vector form factor is kinematically suppressed in this region and can never give such a strong enhancement as observed in these data points.

[2] V. Cirigliano, A. Crivellin and M. Hoferichter, "No-go theorem for nonstandard explanations of the $\tau \to K_S\pi\nu_\tau$ CP asymmetry," Phys. Rev. Lett. **120** (2018) no.14, 141803.

[3] H. Z. Devi, L. Dhargyal and N. Sinha, "Can the observed CP asymmetry in $\tau \to K\pi\nu_\tau$ be due to nonstandard tensor interactions?," Phys. Rev. D **90** (2014) no.1, 013016.

[4] L. Dhargyal, "Full angular spectrum analysis of tensor current contribution to $A_{cp}(\tau \to K_s\pi\nu_\tau)$," LHEP **1**, no.3, 9-14 (2018).

[5] L. Dhargyal, "New tensor interaction as the source of the observed CP asymmetry in $\tau \to K_S\pi\nu_\tau$," Springer Proc. Phys. **203** (2018) 329.

[6] J. P. Lees *et al.* [BaBar Collaboration], "Search for CP Violation in the Decay $\tau^- - > \pi^- K^0_S(>= 0\pi^0)\nu_\tau$," Phys. Rev. D **85** (2012) 031102 Erratum: [Phys. Rev. D **85** (2012) 099904].

[7] I. I. Bigi and A. I. Sanda, "A 'Known' CP asymmetry in tau decays," Phys. Lett. B **625** (2005) 47.

[8] G. Calderón, D. Delepine and G. L. Castro, "Is there a paradox in CP asymmetries of $\tau^\pm \to K_{L,S}\pi^\pm\nu_\tau$ decays?," Phys. Rev. D **75** (2007) 076001.

[9] M. Tanabashi *et al.* [Particle Data Group], "Review of Particle Physics," Phys. Rev. D **98**, no. 3, 030001 (2018).

[10] Y. Grossman and Y. Nir, "CP Violation in $\tau \to \nu\pi K_S$ and $D \to \pi K_S$: The Importance of $K_S - K_L$ Interference," JHEP **1204** (2012) 002.

[11] M. Kobayashi and T. Maskawa, "CP Violation in the Renormalizable Theory of Weak Interaction," Prog. Theor. Phys. **49** (1973), 652-657.

[12] A. D. Sakharov, "Violation of CP Invariance, C asymmetry, and baryon asymmetry of the universe," Pisma Zh. Eksp. Teor. Fiz. **5** (1967) 32 [JETP Lett. **5** (1967) 24] [Sov. Phys. Usp. **34** (1991) no.5, 392] [Usp. Fiz. Nauk **161** (1991) no.5, 61].

[13] A. G. Cohen, D. B. Kaplan and A. E. Nelson, "Progress in electroweak baryogenesis," Ann. Rev. Nucl. Part. Sci. **43** (1993) 27.

[14] A. Riotto and M. Trodden, "Recent progress in baryogenesis," Ann. Rev. Nucl. Part. Sci. **49** (1999) 35.

[15] M. Bischofberger *et al.* [Belle Collaboration], "Search for CP violation in $\tau \to K^0_S\pi\nu_\tau$ decays at Belle," Phys. Rev. Lett. **107** (2011) 131801.

[16] D. Epifanov *et al.* [Belle Collaboration], "Study of $\tau^- \to K_S\pi^-\nu_\tau$ decay at Belle," Phys. Lett. B **654** (2007) 65.

[17] B. Moussallam, "Analyticity constraints on the strangeness changing vector current and applications to $\tau^- \to K\pi\nu_\tau$, $\tau \to K\pi\pi\nu_\tau$," Eur. Phys. J. C **53** (2008) 401.

[18] M. Jamin, A. Pich and J. Portolés, "What can be learned from the Belle spectrum for the decay $\tau^- \to \nu_\tau K_S \pi^-$," Phys. Lett. B **664** (2008) 78.

[19] D. R. Boito, R. Escribano and M. Jamin, "K pi vector form-factor, dispersive constraints and $\tau^- \to \nu_\tau K\pi$ decays," Eur. Phys. J. C **59** (2009) 821.

[20] D. R. Boito, R. Escribano and M. Jamin, "K π vector form factor constrained by $\tau- > K\pi\nu_\tau$ and K_{l3} decays," JHEP **1009** (2010) 031.

[21] M. Antonelli, V. Cirigliano, A. Lusiani and E. Passemar. "Predicting the τ strange branching ratios and implications for V_{us}". JHEP 1310 (2013) 070.

[22] D. Kimura, K. Y. Lee and T. Morozumi, "The Form factors of $\tau \to K\pi(\eta)\nu$ and the predictions for CP violation beyond the standard model," PTEP **2013** (2013) 053B03 Erratum: [PTEP **2014** (2014) no.8, 089202].

[23] V. Bernard, "First determination of $f_+(0)|V_{us}|$ from a combined analysis of $\tau \to K\pi\nu_\tau$ decay and πK scattering with constraints from $K_{\ell 3}$ decays," JHEP **1406** (2014) 082.

[24] R. Escribano, S. González-Solís, M. Jamin and P. Roig, "Combined analysis of the decays $\tau^- \to K_S\pi^-\nu_\tau$ and $\tau^- \to K^-\eta\nu_\tau$," JHEP **1409** (2014) 042.

[25] M. Jamin, A. Pich and J. Portolés, "Spectral distribution for the decay $\tau^- \to \nu_\tau K\pi$," Phys. Lett. B **640** (2006) 176.

[26] L. A. Jiménez Pérez and G. Toledo Sánchez, "Absorptive corrections for vector mesons: matching to complex mass scheme and longitudinal corrections," J. Phys. G **44** (2017) no.12, 125003.

[27] E. A. Garcés, M. Hernández Villanueva, G. López Castro and P. Roig, "Effective-field theory analysis of the $\tau^- \to \eta^{(\prime)}\pi^-\nu_\tau$ decays," JHEP **1712** (2017) 027.

[28] J. A. Miranda and P. Roig, "Effective-field theory analysis of the $\tau^- \to \pi^-\pi^0\nu_\tau$ decays," JHEP **11**, 038 (2018).

[29] V. Cirigliano, A. Falkowski, M. González-Alonso and A. Rodríguez-Sánchez, "Hadronic tau decays as New Physics probes in the LHC era," Phys. Rev. Lett. **122** (2019) no.22, 221801.

[30] V. Cirigliano, J. Jenkins and M. González-Alonso, "Semileptonic decays of light quarks beyond the Standard Model," Nucl. Phys. B **830** (2010), 95-115.

[31] T. Bhattacharya, V. Cirigliano, S. D. Cohen, A. Filipuzzi, M. González-Alonso, M. L. Graesser, R. Gupta and H. W. Lin, "Probing Novel Scalar and Tensor Interactions from (Ultra)Cold Neutrons to the LHC," Phys. Rev. D **85**, 054512 (2012).

[32] V. Cirigliano, M. González-Alonso and M. L. Graesser, "Non-standard Charged Current Interactions: beta decays versus the LHC," JHEP **1302** (2013) 046.

[33] V. Cirigliano, S. Gardner and B. Holstein, "Beta Decays and Non-Standard Interactions in the LHC Era," Prog. Part. Nucl. Phys. **71** (2013) 93.

[34] H. M. Chang, M. González-Alonso and J. Martín Camalich, "Nonstandard Semileptonic Hyperon Decays," Phys. Rev. Lett. **114** (2015) no.16, 161802.

[35] A. Courtoy, S. Baessler, M. González-Alonso and S. Liuti, "Beyond-Standard-Model Tensor Interaction and Hadron Phenomenology," Phys. Rev. Lett. **115** (2015) 162001.

[36] M. González-Alonso and J. Martín Camalich, "Global Effective-Field-Theory analysis of New-Physics effects in (semi)leptonic kaon decays," JHEP **1612** (2016) 052.

[37] M. González-Alonso and J. Martín Camalich, "New Physics in $s \to u\ell^-\bar{\nu}$: Interplay between semileptonic kaon and hyperon decays," arXiv:1606.06037 [hep-ph].

[38] S. Alioli, V. Cirigliano, W. Dekens, J. de Vries and E. Mereghetti, "Right-handed charged currents in the era of the Large Hadron Collider," JHEP **1705** (2017) 086.

[39] M. González-Alonso, O. Naviliat-Cuncic and N. Severijns, "New physics searches in nuclear and neutron β decay," Prog. Part. Nucl. Phys. **104** (2019) 165.

[40] M. González-Alonso, J. Martín Camalich and K. Mimouni, "Renormalization-group evolution of new physics contributions to (semi)leptonic meson decays," Phys. Lett. B **772** (2017), 777-785.

[41] B. Grzadkowski, M. Iskrzynski, M. Misiak and J. Rosiek, "Dimension-Six Terms in the Standard Model Lagrangian," JHEP **10**, 085 (2010).

[42] W. Buchmuller and D. Wyler, "Effective Lagrangian Analysis of New Interactions and Flavor Conservation," Nucl. Phys. B **268**, 621-653 (1986).

[43] J. Gasser and H. Leutwyler, "Chiral Perturbation Theory to One Loop," Annals Phys. **158**, 142 (1984).

[44] J. Gasser and H. Leutwyler, "Chiral Perturbation Theory: Expansions in the Mass of the Strange Quark," Nucl. Phys. B **250**, 465-516 (1985).

[45] G. Ecker, J. Gasser, A. Pich and E. de Rafael, "The Role of Resonances in Chiral Perturbation Theory," Nucl. Phys. B **321**, 311-342 (1989).

[46] G. Ecker, J. Gasser, H. Leutwyler, A. Pich and E. de Rafael, "Chiral Lagrangians for Massive Spin 1 Fields," Phys. Lett. B **223**, 425-432 (1989).

[47] A. Sirlin, "Radiative corrections to g(v)/g(mu) in simple extensions of the su(2) x u(1) gauge model," Nucl. Phys. B **71** (1974) 29.

[48] A. Sirlin, "Current Algebra Formulation of Radiative Corrections in Gauge Theories and the Universality of the Weak Interactions," Rev. Mod. Phys. **50** (1978) 573 Erratum: [Rev. Mod. Phys. **50** (1978) 905].

[49] A. Sirlin, "Large m(W), m(Z) Behavior of the O(alpha) Corrections to Semileptonic Processes Mediated by W," Nucl. Phys. B **196** (1982) 83.

[50] W. J. Marciano and A. Sirlin, "Radiative Corrections to beta Decay and the Possibility of a Fourth Generation," Phys. Rev. Lett. **56** (1986) 22.

[51] W. J. Marciano and A. Sirlin, "Electroweak Radiative Corrections to tau Decay," Phys. Rev. Lett. **61** (1988) 1815.

[52] W. J. Marciano and A. Sirlin, "Radiative corrections to pi(lepton 2) decays," Phys. Rev. Lett. **71** (1993) 3629.

[53] E. Braaten and C. S. Li, "Electroweak radiative corrections to the semihadronic decay rate of the tau lepton," Phys. Rev. D **42** (1990) 3888.

[54] J. Erler, "Electroweak radiative corrections to semileptonic tau decays," Rev. Mex. Fis. **50** (2004) 200.

[55] R. Escribano, S. González-Solís, M. Jamin and P. Roig, "Combined analysis of the decays $\tau^- \to K_S\pi^-\nu_\tau$ and $\tau^- \to K^-\eta\nu_\tau$," JHEP **1409** (2014) 042.

[56] M. Jamin, J. A. Oller and A. Pich, "Strangeness changing scalar form-factors," Nucl. Phys. B **622** (2002) 279.

[57] M. Jamin, J. A. Oller and A. Pich, "S wave K pi scattering in chiral perturbation theory with resonances," Nucl. Phys. B **587** (2000) 331.

[58] M. Jamin, J. A. Oller and A. Pich, "Light quark masses from scalar sum rules," Eur. Phys. J. C **24** (2002) 237.

[59] M. Jamin, J. A. Oller and A. Pich, "Order p^6 chiral couplings from the scalar $K\pi$ form-factor," JHEP **0402** (2004) 047.

[60] M. Jamin, J. A. Oller and A. Pich, "Scalar K pi form factor and light quark masses," Phys. Rev. D **74** (2006) 074009.

[61] O. Shekhovtsova, T. Przedzinski, P. Roig and Z. Was, "Resonance chiral Lagrangian currents and τ decay Monte Carlo," Phys. Rev. D **86** (2012), 113008.

[62] O. Catà and V. Mateu, "Chiral perturbation theory with tensor sources," JHEP **09**, 078 (2007).

[63] A. Guevara, P. Roig and J. J. Sanz-Cillero, "Pseudoscalar pole light-by-light contributions to the muon $(g-2)$ in Resonance Chiral Theory," JHEP **06** (2018), 160.

[64] R. Escribano, S. Gonzàlez-Solís and P. Roig, "Predictions on the second-class current decays $\tau^- \to \pi^-\eta^{(\prime)}\nu_\tau$," Phys. Rev. D **94** (2016) no.3, 034008.

[65] I. Baum, V. Lubicz, G. Martinelli, L. Orifici and S. Simula, "Matrix elements of the electromagnetic operator between kaon and pion states," Phys. Rev. D **84**, 074503 (2011).

[66] S. Gonzàlez-Solís and P. Roig, "A dispersive analysis of the pion vector form factor and $\tau^- \to K^- K_S \nu_\tau$ decay," Eur. Phys. J. C **79** (2019) no.5, 436.

[67] E. Kou *et al.* [Belle-II], "The Belle II Physics Book," PTEP **2019**, no.12, 123C01 (2019) [erratum: PTEP **2020**, no.2, 029201 (2020)].

[68] L. Beldjoudi and T. N. Truong, "tau to pi K neutrino decay and pi K scattering," Phys. Lett. B **351** (1995) 357.

[69] D. N. Gao and X. F. Wang, "On the angular distributions of $\tau^- \to K_S \pi^- \nu_\tau$ decay," Phys. Rev. D **87** (2013) 073016.

[70] Y. Amhis *et al.* [HFLAV Collaboration], "Averages of b-hadron, c-hadron, and τ-lepton properties as of summer 2016," Eur. Phys. J. C **77** (2017) no.12, 895.

[71] P. Roig, "Semileptonic τ decays: powerful probes of non-standard charged current weak interactions," EPJ Web Conf. **212** (2019), 08002.

[72] F. Z. Chen, X. Q. Li, Y. D. Yang and X. Zhang, "CP asymmetry in $\tau \to K_S \pi \nu_\tau$ decays within the Standard Model and beyond," Phys. Rev. D **100**, no.11, 113006 (2019).

[73] F. Z. Chen, X. Q. Li and Y. D. Yang, "CP asymmetry in the angular distribution of $\tau \to K_S \pi \nu_\tau$ decays," JHEP **05**, 151 (2020).

[74] F. Z. Chen, X. Q. Li, S. C. Peng, Y. D. Yang and H. H. Zhang, "CP asymmetry in the angular distributions of $\tau \to K_S \pi \nu_\tau$ decays – II: general effective field theory analysis," [arXiv:2107.12310 [hep-ph]].